Contribution from Amoco Chemical Company,
Amoco Research Center, Naperville, Illinois 60566

Synthesis of Isopolymetalate-Pillared Hydrotalcite via Organic-Anion-Pillared Precursors

Mark A. Drezdzon

Received July 6, 1988

Organic-anion-pillared hydrotalcites such as $Mg_4Al_2(OH)_{12}(TA)\cdot xH_2O$ (TA = terephthalate) are easily synthesized by using coprecipitation/digestion techniques. Exchange of these materials under mildly acidic conditions with the appropriate metalate proceeds smoothly to yield multihundred-gram samples of $Mg_{12}Al_6(OH)_{36}(Mo_7O_{24})\cdot xH_2O$ and $Mg_{12}Al_6(OH)_{36}(V_{10}O_{28})\cdot xH_2O$. These isopolymetalate-pillared hydrotalcites exhibit thermal stability to over 500 °C in air.

Introduction

An extensively studied class of inorganic materials for use in catalytic applications is the smectite clays.[1-3] These materials comprise negatively charged metal silicate sheets intercalated or pillared with hydrated cations. By use of well-established ion-exchange techniques, a wide variety of cations may be incorporated into clays such as montmorillonite.[2-7] Through changes in the size of the pillar used to separate the sheets in the clay structure, the pore size of the pillared clay may be tailored to a particular application.[3]

The main obstacle encountered in trying to synthesize useful molecular-sieve-like compounds from clays has been the stability of the pillar. Pillared clays intercalated with organic-based cations and metal complexes decompose below 250 and 450 °C, respectively, due to degradation of the organic material.[3-5] However, with the use of polynuclear hydroxymetal cations as the pillaring species, porous clay materials can be made that are stable above 500 °C.[3,7] Also, the pillars in transition metal halide cluster pillared clays are oxidized by water at 240 °C to form stable metal oxide pillars.[6]

Although polynuclear transition metal halide and hydroxymetal cations yield thermally stable pillared clays, the number of such species is limited. The negatively charged polyoxometalates[8] present a wider range of thermally stable, catalytically active pillars, provided a suitable host material is utilized.

One class of suitable host materials for polyoxometalate pillars is the naturally occurring hydrotalcite-type materials.[9] The structure of hydrotalcite, $Mg_6Al_2(OH)_{16}(CO_3)\cdot 4H_2O$, is derived from brucite, $Mg(OH)_2$, by isomorphous replacement of some of the octahedrally coordinated divalent magnesium cations with trivalent cations.[10,11] The resulting positive charge on the metal hydroxide sheets (or brucite layers) is balanced by intercalation of carbonate into the interlayer region of the structure. Hydrotalcite-type clays incorporating a wide variety of divalent and trivalent cations, cation ratios, and interlayer anions have been synthesized and characterized both structurally and catalytically (Figure 1).[11-14]

This paper describes work culminating in the synthesis of heptamolybdate- and decavanadate-pillared hydrotalcite-type clays. The novel approach taken in synthesizing these materials has been to prepare an organic-anion-pillared clay precursor that is subsequently exchanged with the appropriate isopolymetalate under mildly acidic conditions (Figure 2). Here, the brucite layers are widely separated by the large organic anions prior to isopolymetalate exchange. This approach differs from those previously reported in the field[15,16] where chloride-containing hydrotalcites were exchanged with polyoxometalates.

Experimental Section

Materials and Methods. The reagents, NaOH (Fisher), $Mg(NO_3)_2\cdot 6H_2O$ (Alfa), $Al(NO_3)_3\cdot 9H_2O$ (Alfa), terephthalic acid (Amoco), $Na_2MoO_4\cdot 2H_2O$ (Strem), and $NaVO_3$ (Alfa), were used as received.

Powder X-ray diffraction patterns were obtained by using a Philips diffractometer automated with a Nicolet L-11 system. An external

(1) (a) He, M.; Liu, Z.; Min, E. *Catal. Today* **1988**, *2*, 321. (b) Laszlo, P. *Science (Washington, D.C.)* **1987**, *235*, 1473. (c) Cornelis, A.; Laszlo, P. *NATO ASI Ser., Ser. C* **1986**, *165*, 213. (d) Ballantine, J. A. *NATO ASI Ser., Ser. C* **1986**, *165*, 197. (e) Pinnavaia, T. J. *NATO ASI Ser., Ser. C* **1986**, *165*, 151. (f) Jones, W.; Thomas, J. M.; Tennakoon, T. B.; Schlogl, R.; Diddams, P. *ACS Symp. Ser.* **1985**, *No. 288*, 472. (g) Occelli, M. L.; Landau, S. D.; Pinnavaia, T. J. *J. Catal.* **1984**, *90*, 256. (h) Occelli, M. L. *Ind. Eng. Chem. Prod. Res. Dev.* **1983**, *22*, 553. (i) Occelli, M. L.; Tindwa, R. M. *Clays Clay Miner.* **1983**, *31*, 22. (j) Shabtai, J.; Lazar, R.; Oblad, A. G. *Stud. Surf. Sci. Catal.* **1981**, *7*, 828. (k) Weiss, A. *Angew. Chem., Int. Ed. Engl.* **1981**, *20*, 850.

(2) (a) Adams, J. M. *Appl. Clay Sci.* **1987**, *2*, 309. (b) Barrer, R. M. *Stud. Surf. Sci. Catal.* **1986**, *28*, 3. (c) Maes, A.; Cremers, A. *ACS Symp. Ser.* **1986**, *No. 323*, 254. (d) Adams, J. M.; Ballantine, J. A.; Graham, S. H.; Laub, R. J.; Purnell, J. H.; Reid, P. I.; Shaman, W. Y. M.; Thomas, J. M. *J. Catal.* **1979**, *58*, 238.

(3) (a) Pinnavaia, T. J. *Science (Washington, D.C.)* **1983**, *220*, 365. (b) Barrer, R. M. *Zeolites and Clay Minerals as Sorbents and Molecular Sieves*; Academic: New York, 1978.

(4) Mortland, M. M.; Berkheiser, V. E. *Clays Clay Miner.* **1976**, *24*, 60.

(5) (a) Raythatha, R.; Pinnavaia, T. J. *J. Catal.* **1983**, *80*, 47. (b) Pinnavaia, T. J. *ACS Symp. Ser.* **1982**, *No. 192*, 241. (c) Pinnavaia, T. J.; Raythatha, R.; Lee, J. G.-S.; Halloran, C. J.; Hoffman, J. F. *J. Am. Chem. Soc.* **1979**, *101*, 6891. (d) Traynor, M. F.; Mortland, M. M.; Pinnavaia, T. J. *Clays Clay Miner.* **1978**, *26*, 319. (e) Thomas, J. M.; Adams, J. M.; Graham, S. H.; Tennakoon, T. B. *Adv. Chem. Ser.* **1977**, *No. 163*, 298. (f) Knudson, M. I.; McAtee, J. L. *Clays Clay Miner.* **1973**, *21*, 19.

(6) Christiano, S. P.; Wang, J.; Pinnavaia, T. J. *Inorg. Chem.* **1985**, *24*, 1222.

(7) (a) Carrado, K. A.; Suib, S. L.; Skoularikis, N. D.; Coughlin, R. W. *Inorg. Chem.* **1986**, *25*, 4217. (b) Pinnavaia, T. J.; Tzou, M.-S.; Landau, S. D. *J. Am. Chem. Soc.* **1985**, *107*, 4783. (c) Pinnavaia, T. J.; Tzou, N.-S.; Landau, S. D.; Rasik, H. R. *J. Mol. Catal.* **1984**, *27*, 195. (d) Yamanaka, S.; Brindley, G. W. *Clays Clay Miner.* **1979**, *27*, 119. (e) Yamanaka, S.; Brindley, G. W. *Clays Clay Miner.* **1978**, *26*, 21. (f) Lahav, N.; Shani, U.; Shabtai, J. *Clays Clay Miner.* **1978**, *26*, 107. (g) Brindley, G. W.; Samples, R. E. *Clay Miner.* **1977**, *12*, 229.

(8) Pope, M. T. *Heteropoly and Isopoly Oxometalates*; Springer-Verlag: New York, 1983.

(9) (a) Taylor, H. F. W. *Mineral. Mag.* **1973**, *39*, 377. (b) Pastor-Rodriguez, J.; Taylor, H. F. W. *Mineral. Mag.* **1971**, *38*, 286. (c) De Waal, S. A.; Viljoen, E. A. *Am. Mineral.* **1971**, *56*, 1077. (d) Ingram, L.; Taylor, H. F. W. *Mineral. Mag.* **1967**, *36*, 465.

(10) (a) Allmann, R.; Jepsen, H. P. *Neues Jahrb. Mineral. Monatsh.* **1969**, *11*, 544. (b) Allmann, R. *Acta Crystallogr.* **1968**, *B24*, 972. (c) Allmann, R.; Lohse, H. H. *Neues Jahrb. Mineral. Monatsch.* **1966**, *11*, 161. (d) Frondel, C. *Am. Mineral.* **1941**, *26*, 295.

(11) (a) Ross, G. J.; Kodama, H. *Am. Mineral.* **1967**, *52*, 1036. (b) Brown, G.; Gastuche, M. C. *Clay Miner.* **1967**, *7*, 193. (c) Gastuche, M. C.; Herbillon, A. *Bull. Soc. Chim. Fr.* **1962**, *16*, 1404.

(12) (a) Taylor, R. M. *Clay Miner.* **1984**, *19*, 591. (b) Brindley, G. W.; Kao, C.-C. *Phys. Chem. Miner.* **1984**, *10*, 187. (c) Brindley, G. W.; Kikkawa, S. *Clays Clay Miner.* **1980**, *28*, 87. (d) Miyata, S. *Clays Clay Miner.* **1980**, *28*, 50. (e) Miyata, S.; Okada, A. *Clays. Clay Miner.* **1977**, *25*, 14. (f) Miyata; S. *Clays Clay Miner.* **1975**, *23*, 369.

(13) (a) Sambrook, R. M.; Ross, J. R. H. U.S. Patent 4 530 918 (to Dyson Refractories Limited), July 23, 1985. (b) Reichle, W. T. U.S. Patent 4 476 324 (to Union Carbide Corp.), Oct 9, 1984. (c) Reichle, W. T. U.S. Patent 4 458 026 (to Union Carbide Corp.), July 3, 1984. (d) Reichle, W. T. U.S. Patent 4 086 188 (to Union Carbide Corp.), April 25, 1978. (e) Miyata, S.; Kumura, T.; Shimada, M. U.S. Patent 3 879 525 (to Kyowa Chemical Industry Co., Ltd.), April 22, 1975. (f) Miyata, S.; Kumura, T.; Shimada, M. U.S. Patent 3 879 523 (to Kyowa Chemical Industry Co., Ltd.), April 22, 1975. (g) Miyata, S.; Kumura, T.; Shimada, M. U.S. Patent 3 796 792 (to Kyowa Chemical Industry Co., Ltd.), March 12, 1974.

(14) (a) Reichle, W. T. *CHEMTECH* **1986**, 58. (b) Reichle, W. T.; Kang, S. Y.; Everhardt, D. S. *J. Catal.* **1986**, *101*, 352. (c) Reichle, W. T. *J. Catal.* **1985**, *94*, 547. (d) Nakatsuka, T.; Kawasaki, H.; Yamashita, S.; Kohjiya, S. *Bull. Chem. Soc. Jpn.* **1979**, *52*, 2449.

(15) (a) Iyagba, E. T. Thesis, University of Pittsburgh, Pittsburgh, PA, 1986. (b) Woltermann, G. M. U.S. Patent 4 454 244 (to Ashland Oil, Inc.), June 12, 1984.

(16) Kwon, T.; Tsigdinos, G. A.; Pinnavaia, T. J. *J. Am. Chem. Soc.* **1988**, *110*, 3653.

0020-1669/88/1327-4628$01.50/0

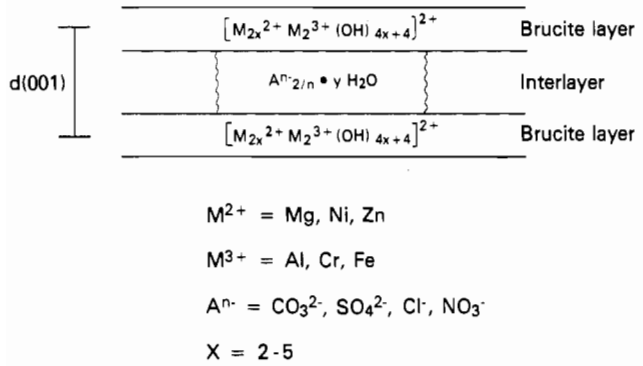

Figure 1. Schematic representation of hydrotalcite-type clays.

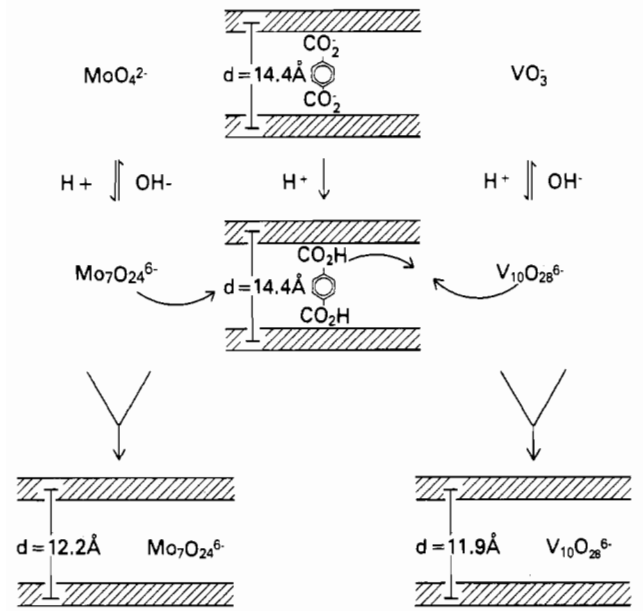

Figure 2. Schematic representation of terephthalate exchange with heptamolybdate and decavanadate in hydrotalcite. Clay *d* spacings were calculated from models.

standard (Si) was used to verify peak positions. A fine-focus Cu tube, operated at 40 kV and 20 mA, was the X-ray source, and a 4° fixed divergence slit, 0.2° receiving slit, and diffracted-beam monochromator were used. Samples were step-scanned from 6 to 70° 2θ in 0.04° steps with a counting time of 1 s/step.

Clay specimens for preferred-orientation X-ray diffraction (POXRD) were prepared by evaporating dilute aqueous clay slurries (1–2 wt % clay) onto microscope slides. Patterns were obtained on a GE/Diano XRD-5 diffractometer automated with a Nicolet L-11 system. An external standard (Si) was used to verify peak positions. Ni-filtered Cu Kα radiation (50 kV, 16 mA) was used with a 3° divergence slit and a 0.2° scattering slit. Samples were step-scanned from 3 to 70° 2θ in 0.4° steps with a counting time of 16 s/step.

TEM micrographs were taken on a Philips 400T electron microscope operated at 120 kV. Specimens were prepared by grinding the sample to a fine powder, dispersing in epoxy resin, and shaving thin sections from the hardened epoxy block with a microtome. SEM micrographs were obtained on a Philips 501 SEM instrument using clay samples dispersed in ethanol, sprayed on a foil-covered stub and then C/Au coated by evaporation.

Thermal analyses (DTA/TGA) were done on a Du Pont 9900 thermal analysis system. BET (N_2) surface areas were determined on a Quantachrome Autosorb-6.

One-dimensional electron density maps were calculated by using standard techniques.[17] Maps for model systems were determined by a calculation of the theoretical (00*l*) diffraction pattern, followed by a 1-D electron density map calculation using the calculated (001) through (004) diffraction peaks.[17] This allows direct comparison with experimentally determined electron density maps (usually calculated from (001) through (004) lines).

(17) Stout, G. H.; Jensen, L. H. *X-Ray Structure Determination*; Macmillan: New York, 1968.

Synthesis of $Mg_4Al_2(OH)_{12}(TA)\cdot xH_2O$ (TA = Terephthalate Dianion). A 5-L, three-neck, round-bottom flask equipped with a reflux condenser, thermometer, mechanical stirrer, and electric heating mantle was charged with 1600 mL of deionized water, 133.1 g of terephthalic acid (0.801 mol), and 575 g of 50% NaOH solution (7.19 mol). While this mixture was stirred and cooled to room temperature, a solution containing 1280 mL of deionized water, 410.1 g of $Mg(NO_3)_2\cdot H_2O$ (1.60 mol), and 300.0 g of $Al(NO_3)_3\cdot 9H_2O$ (0.800 mol) was prepared in a separate beaker. The metal nitrate solution was then added dropwise to the vigorously stirred terephthalate/NaOH solution at room temperature over a period of 90 min. After complete addition of the metal nitrate solution, the gellike mixture was digested at 73–74 °C for 18 h. Upon cooling, the product was isolated by filtration until most of the water had been removed; the filter cake was not allowed to suction to dryness.[18] The product was washed by reslurrying with 2 L of fresh deionized water and stored in a 1-gal jar. The final slurry (2790 g) contained 7.39 wt % clay (net weight of clay = 203 g, 86% yield).

POXRD: 2θ = 6.01° (001), 12.10° (002), 18.45° (003), 24.70° (004); *d* spacing = 14.4 Å. Anal. Calcd for $Mg_{4.27}Al_2(OH)_{12.54}(TA)\cdot 4H_2O$: Mg, 17.09; Al, 8.89; C, 15.82. Found: Mg, 16.93; Al, 8.80; C, 15.50. TGA up to 350 °C revealed a sample weight loss of 10.5% (calcd for loss of $4H_2O$: 11.9%). SEM revealed a homogeneous matrix of slightly flattened beadlike particles approximately 1000–2000 Å in diameter. BET surface area = 35 m^2/g, which increased to 298 m^2/g after calcination at 500 °C for 12 h.

Synthesis of $Mg_{12}Al_6(OH)_{36}(Mo_7O_{24})\cdot xH_2O$. To a 2500-g portion of the preceding $Mg_{4.27}Al_2(OH)_{12.54}(TA)$–clay slurry was added a solution consisting of 254 g of $Na_2MoO_4\cdot 2H_2O$ (1.05 mol) in 450 mL of deionized water. The amount of molybdate added corresponds to a 50% excess of that needed for stoichiometric exchange of terephthalate with $Mo_7O_{24}^{6-}$. After the mixture was stirred for 10–15 min, approximately 350 mL of 4 N HNO_3 was slowly added to the mixture with vigorous stirring, resulting in a pH drop from 12.0 to 4.4. After 5 min of additional stirring (pH = 4.7), the product was filtered, washed, and dried at 125 °C overnight. The yield of hard, slightly off-white chunks of clay was 215 g (94%).

POXRD: 2θ = 7.1° (001), 14.3° (002), 22.1° (003); *d* spacing = 12.17 Å. Anal. Calcd for $Mg_{12.26}Al_6(OH)_{36.52}(Mo_7O_{24})\cdot 6H_2O$: Mg, 13.28; Al, 7.21; Mo, 29.92. Found: Mg, 13.25; Al, 7.20; Mo, 28.70; C, 1.62. TGA up to 350 °C revealed a sample weight loss of 3.2% (calcd: for loss of $4H_2O$, 3.3%; for loss of $6H_2O$, 4.8%). SEM revealed a homogeneous matrix of beadlike particles approximately 1000–2000 Å in diameter. BET surface area = 27 m^2/g, which increased to 32 m^2/g after calcination at 500 °C for 12 h.

Synthesis of $Mg_{12}Al_6(OH)_{36}(V_{10}O_{28})\cdot xH_2O$. To a 1400-g portion of an $Mg_4Al_2(OH)_{12}(TA)\cdot xH_2O$ clay was added a solution consisting of 73.91 g of $NaVO_3$ (0.606 mol) in 500 mL of deionized water. The amount of vanadate added corresponds to a 50% excess of that needed for stoichiometric exchange of terephthalate with $V_{10}O_{28}^{6-}$. After the mixture was stirred for 10–15 min, approximately 320 mL of 2 N HNO_3 was slowly added to the mixture with vigorous stirring, resulting in a pH drop from 9.0 to 4.5. After 5 min of additional stirring (pH = 4.9), the product was isolated and worked up as described above. The yield of hard, yellowish chunks of clay was 105 g (85%).

POXRD: 2θ = 7.57° (001), 14.96° (002), 22.60° (003), 30.39° (004); *d* spacing = 11.8 Å. Anal. Calcd for $Mg_{12.83}Al_6(OH)_{37.66}(V_{10}O_{28})\cdot 6H_2O$: Mg, 14.31; Al, 7.43; V, 23.37. Found: Mg, 14.55; Al, 7.56; V, 23.80; C, 0.99. TGA up to 350 °C revealed a sample weight loss of 5.0% (calcd for loss of $6H_2O$: 5.0%). SEM revealed a homogeneous matrix of beadlike particles approximately 1000–2000 Å in diameter. BET surface area = 30 m^2/g, which increased to 32 m^2/g after calcination at 500 °C for 12 h.

Results and Discussion

General Approach. Since hydrotalcite-type clays have higher charge densities, it was expected that they would be more difficult to swell and exchange when compared to typical silicate-based clays.[19] Work by Kikkawa et al.[20] has shown that the anion-exchange reactions of hydrotalcite proceed with greater difficulty as the charge density of the material increases (i.e. as the Mg:Al atomic ratio decreases) due to the increased electrostatic attraction

(18) The terephthalate-pillared hydrotalcite clay intermediate forms a homogeneous slurry in the following exchange step much more readily if the material is kept moist.

(19) For example, montmorillonites typically have exchange capacities on the order of 0.7–1.0 mequiv/g. This is much less than the exchange capacities of 4.1 and 2.4 mequiv/g calculated for $Mg_4Al_2(OH)_{12}CO_3\cdot xH_2O$ and $Mg_{10}Al_2(OH)_{24}CO_3\cdot xH_2O$, respectively.

(20) Kikkawa, S.; Koizumi, M. *Mater. Res. Bull.* **1982**, *17*, 191.

Table I. Comparison of Expected and Observed $d(001)$ Spacings for Hydrotalcite Intercalated with Various Organic Anions

anion	anion size, Å[a]	$d(001)$ spacing, Å	
		expected	obsd[b]
CO_3^{2-}	2.8	7.7	7.7
$[O_2C(CH_2)_2CO_2]^{2-}$	7.9	12.8	7.8
$[O_2C(CH_2)_4CO_2]^{2-}$	10.2	15.1	7.8
$[O_2C(CH_2)_8CO_2]^{2-}$	14.9	19.8	7.8
$[p\text{-}(CO_2)_2C_6H_4]^{2-}$	9.5	14.4	14.4
$[2,5\text{-}(OH)_2\text{-}1,4\text{-}(SO_3)_2C_6H_2]^{2-}$	10.3	15.2	14.7
$[p\text{-}(SO_3)(CH_3)C_6H_4]^{-}$	9.9	14.8	
$[p\text{-}(SO_3)(CH_3)C_6H_4\cdot H_2O]^{-}$	12.7	17.6	17.2
$[1,5\text{-}(SO_3)_2C_{10}H_6]^{2-}$	10.4	15.3	15.1
$CH_3(CH_2)_{11}OSO_3^{-}$	21.3	26.2	26.3

[a] Assumptions: van der Waals radius of O is 1.4 Å and of H is 1.2 Å; anion is oriented with long axis perpendicular to brucite layers. [b] Average values from syntheses starting with a Mg:Al molar ratio of 2:1.

between the brucite layers and the interlayer anions.

In order to avoid the problem of exchanging a relatively small anion, such as carbonate or chloride, with a relatively large polyoxometalate, the synthetic strategy illustrated in Figure 2 was pursued. By use of this strategy, an organic anion may be chosen so that the interlayer distance in the organic-anion-pillared hydrotalcite is slightly larger than that in the incoming polyoxometalate. Acidification of the organic-anion-pillared clay slurry in the presence of monometalate results in oligomerization of the metalate to form a polyoxometalate[8] as well as protonation of the organic anion. Migration of the highly charged polyoxometalate into the interlayer region of the clay in exchange for the organic species results in the final polyoxometalate-pillared hydrotalcite with a slightly smaller d spacing than the organic anion-pillared precursor.

Synthesis of Organic-Anion-Pillared Hydrotalcites. Molecular modeling studies indicated that organic anions containing an aromatic ring would be large enough to properly separate the brucite layers of hydrotalcite for polyoxometalate exchange as described above.[21] Subsequently, a series of hydrotalcite clay syntheses were performed by published procedures[13,14] except for the substitution of the desired organic material for carbonate. In this manner, hydrotalcites pillared with terephthalate, p-toluenesulfonate, 2,5-dihydroxy-1,4-benzenedisulfonate, or 1,5-naphthalenedisulfonate were prepared, as confirmed by elemental analysis and X-ray diffraction (Figure 3).

The d spacings of the organic-anion-pillared hydrotalcites mentioned above agree well with d spacings calculated from models assuming the aromatic ring is perpendicular to the brucite layers (Table I). In the case of p-toluenesulfonate-pillared hydrotalcite, it is proposed that a water molecule is coordinated to the sulfonate group as in p-toluenesulfonic acid monohydrate.

When examined by SEM, organic-anion-pillared hydrotalcite clay samples synthesized by digestion at 65 °C overnight are found to contain slightly flattened beadlike particles approximately 1000–2000 Å in diameter (Figure 4a). Examination of these same samples by TEM at high magnification reveals the layered structure of these materials (Figure 4b). The d spacings measured directly from TEM micrographs agree well with d spacings determined by X-ray diffraction.

Assuming that the space remaining in the interlayer region of organic-anion-pillared hydrotalcites is filled with water, the surface area of dried (125 °C) clay samples should be between 20 and

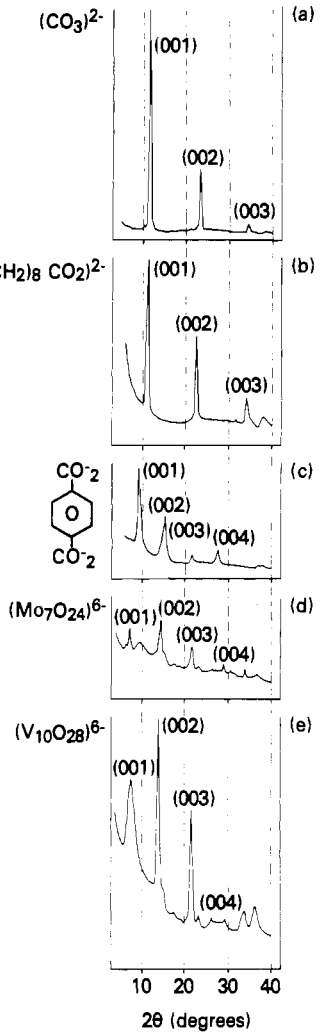

Figure 3. Comparison of POXRD patterns from selected clay syntheses and exchanges. (00l) reflections are labeled: (a) $Mg_4Al_2(OH)_{12}CO_3\cdot 3H_2O$ (d = 7.7 Å); the pattern for the chloride analogue is shifted to slightly lower 2θ values (d = 7.9 Å); (b) attempted synthesis of $Mg_4Al_2(OH)_{12}(O_2C(CH_2)_8CO_2)\cdot xH_2O$ (d = 7.9 Å); the small d spacing indicates the clay is not pillared with sebacate anions (see Table I); (c) $Mg_4Al_2(OH)_{12}(TA)\cdot 4H_2O$ (d = 14.4 Å); (d) $Mg_{12}Al_6(OH)_{36}(Mo_7O_{24})\cdot 6H_2O$ (d = 12.2 Å); (e) $Mg_{12}Al_6(OH)_{36}(V_{10}O_{28})\cdot 6H_2O$ (d = 11.8 Å).

40 m^2/g, corresponding to nonporous spheres 1000–2000 Å in diameter.[22] Surface area measurements (BET/N_2) on organic-anion-pillared hydrotalcites are generally in good agreement with this assessment.

A one-dimensional electron density map calculated from (00l) X-ray diffraction data obtained on a terephthalate-pillared hydrotalcite was compared to a model containing four H_2O molecules per terephthalate anion in the interlayer.[23] On the basis of the small number of observed X-ray diffraction lines, agreement between the experimental data and data obtained from the proposed model is excellent (Figure 5a).

In neutral or basic media, the organic-anion-pillared hydrotalcites are stable indefinitely. Treatment of these materials with monometalate salts (Na_2MoO_4 or $NaVO_3$) without acidification results in no exchange.

(21) This assumes that the aromatic rings will be oriented perpendicular to the brucite layers. On the basis of models, the number of organic anions required in the interlayer for change balance represents >1 monolayer if the anions were to "lie down" between the layers. Since hydrotalcites have relatively high charge densities,[19] it is expected that the anions will "stand up" and form a monolayer instead of forming a bilayer of anions "lying down". This behavior is demonstrated by various smectites, vermiculites, and micas when intercalcated with polar molecules such as amines (see, for example: Lagaly, G.; Weiss, A. *Proc. Int. Clay Conf.* **1969**, *1*, 61).

(22) Assume organic-anion-pillared hydrotalcite clay samples comprise nonporous spheres with density 2.10 g/cm^3 [10] that pack with 74% efficiency (close packed). The surface area is then given by

$$\text{surface area} = 38600/d$$

where the sphere diameter d is in Å and the surface area is in m^2/g.

(23) Electron density maps calculated from hydrotalcite models that do not include water in the interlayer agree poorly with the experimental data. The hydrated models used correspond to an interlayer that is completely stuffed with polyoxometalate pillars and water molecules.

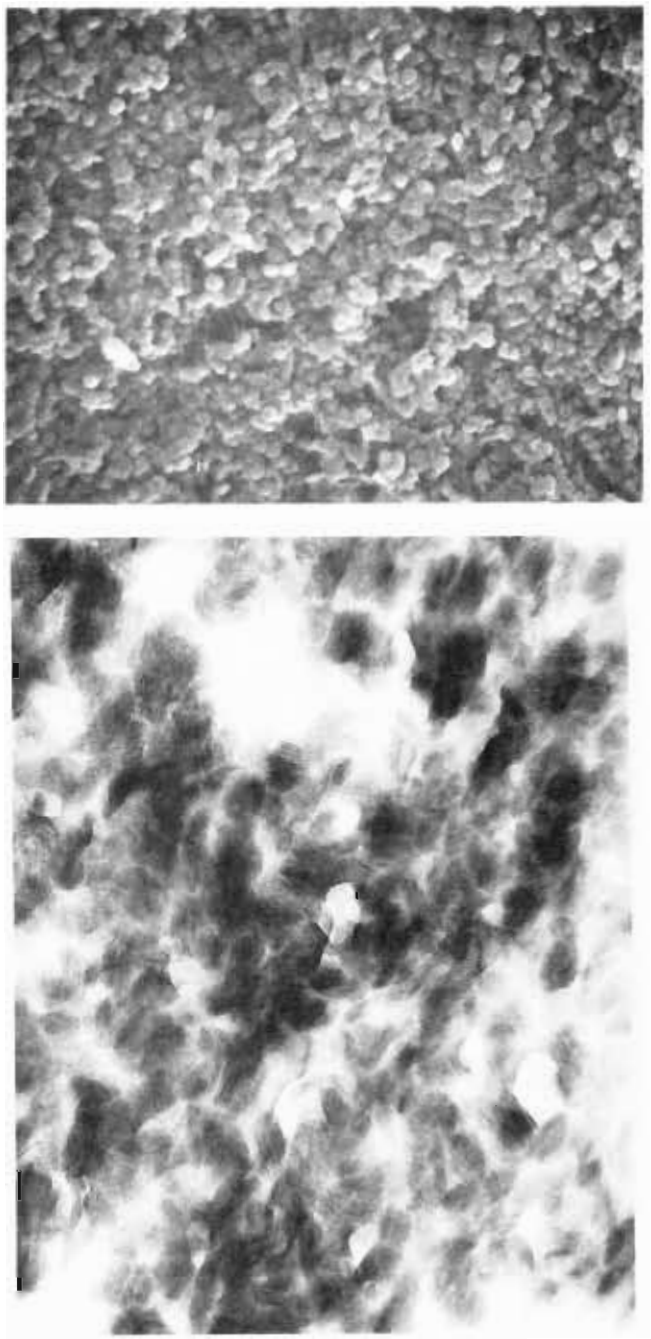

Figure 4. Electron micrographs of two organic anion-pillared hydrotalcite clays: (a, top) SEM micrograph (20000×) of terephthalate-pillared hydrotalcite; individual clay particles are approximately 1000 Å in diameter; (b, bottom) TEM micrograph (200 000×) of *p*-toluenesulfonate-pillared hydrotalcite. Individual layers are approximately 17 Å apart.

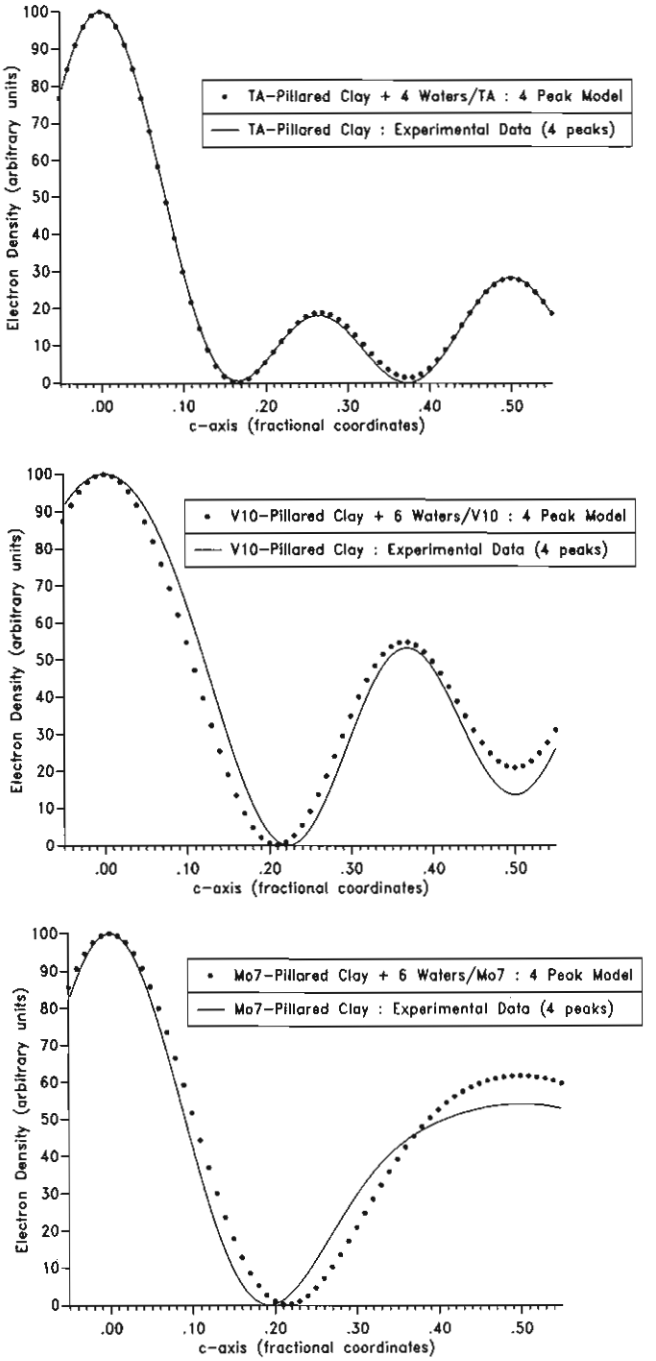

Figure 5. One-dimensional electron density maps for several pillared hydrotalcite clays. Experimental data are compared to fully hydrated model structures: (a, top) $Mg_4Al_2(OH)_{12}(TA)\cdot 4H_2O$; (b, middle) $Mg_{12}Al_6(OH)_{36}(V_{10}O_{28})\cdot 6H_2O$; (c, bottom) $Mg_{12}Al_6(OH)_{36}(Mo_7O_{24})\cdot 6H_2O$.

When terephthalate- or *p*-toluenesulfonate-pillared hydrotalcites are acidified with dilute HCl or HNO_3, collapse of the structure to form the chloride- or nitrate-containing hydrotalcite, respectively, occurs. It is proposed that acidification of the organic-anion-pillared hydrotalcite results in protonation of the organic anion, weakening the electrostatic interaction between the organic species and the brucite layers and allowing migration of the organic species out of the clay interlayer. Collapse of 1,5-naphthalenedisulfonate-pillared hydrotalcite upon acidification proceeds with much greater difficulty, possibly due to slower diffusion rates with the bulkier naphthalene-sized anions as compared to those with the smaller benzene-sized terephthalate and *p*-toluenesulfonate anions. Diffusion problems may also be used to explain the complete resistance of lauryl sulfate pillared hydrotalcite to collapse, wherein entanglement of the long hydrocarbon chains probably prevents diffusion of the anions out of the clay interlayer.

A series of organic-anion-pillared hydrotalcites was reported 15 years ago by Miyata and Kumura in which the organic anions used were linear aliphatic terminal dicarboxylates.[24] Attempts at synthesizing these materials, using digestion conditions identical with those used for successful organic-anion-pillared hydrotalcite clay syntheses, with a variety of brucite layer metals ($M^{2+} = Mg^{2+}$ or Zn^{2+}; $M^{3+} = Al^{3+}$ or Fe^{3+}), metal ratios ($M^{2+}/M^{3+} = 2$–5), and dicarboxylates (succinate, adipate, or sebacate) were unsuccessful, as indicated by X-ray diffraction (Figure 3, Table I)

(24) Miyata, S.; Kumura, T. *Chem. Lett.* **1973**, 843. It is interesting to note that a hydrotalcite clay pillared with adipate anions would result in a structure with a *d* spacing similar to that found for terephthalate-pillared hydrotalcite (Table I).

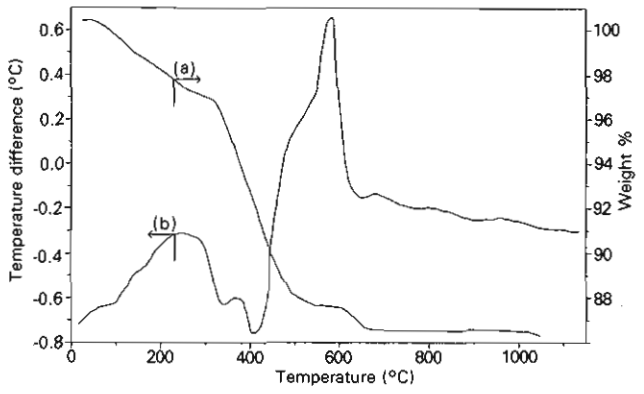

Figure 6. Thermal analysis data for $Mg_{12}Al_6(OH)_{36}(Mo_7O_{24})\cdot 6H_2O$: (a) TGA; (b) DTA.

and elemental analysis. The failure of these syntheses may be due to the use of different digestion conditions not specified in the publication. However, hydrotalcite pillared with the long-chain sulfate $CH_3(CH_2)_{11}OSO_3^-$ was successfully prepared by using our digestion conditions (Table I). This lauryl sulfate pillared hydrotalcite has also been reported by Iyagba.[15a]

Synthesis of Isopolymetalate-Pillared Hydrotalcites. Exchange of terephthalate-pillared hydrotalcite with molybdate or vanadate under mildly acidic conditions proceeds smoothly to yield heptamolybdate- or decavanadate-pillared hydrotalcite, respectively, as indicated by X-ray diffraction (Figure 3) and elemental analysis. These same products are obtained upon exchange of *p*-toluenesulfonate-pillared hydrotalcite under identical conditions. The *d* spacing of the heptamolybdate-pillared hydrotalcite (d = 12.2 Å) corresponds to a $Mo_7O_{24}^{6-}$ orientation in which the C_2 axis is perpendicular to the brucite layers. In the case of decavanadate-pillared hydrotalcite, the *d* spacing (11.9 Å) corresponds to a $V_{10}O_{28}^{6-}$ orientation in which the C_2 axis is parallel to the brucite layers. In both cases, the shortest dimension of the isopolymetalate is perpendicular to the brucite layers, affording the product with the lowest free energy.

Exchange reactions using the 2,5-dihydroxy-1,4-benzenedisulfonate-pillared hydrotalcite precursor yield heterogeneous products. This exchange reaction may be complicated by complex formation between the organic species and metalate.[25] Exchange reactions with other organic-anion-pillared hydrotalcites proceed with difficulty (1,5-naphthalenedisulfonate) or do not proceed at all (lauryl sulfate), as expected from the acidification studies described in the previous section.

Examination of isopolymetalate-pillared hydrotalcites by SEM reveals particles identical in appearance with those of the organic-anion-pillared hydrotalcite clay precursor (Figure 6a). Also, surface area data (BET/N_2) on isopolymetalate-pillared hydrotalcites agree well with surface areas predicted for nonporous spheres 1000–2000 Å in diameter.[22]

One-dimensional electron density maps calculated from (00*l*) X-ray diffraction data obtained on isopolymetalate-pillared hydrotalcites were compared to models containing six H_2O molecules per isopolymetalate anion in the interlayer.[23] Although agreement between the experimental data and data obtained from the proposed models is not as good as for the terephthalate-pillared

(25) Intorre, B. I.; Martell, A. E. *J. Am. Chem. Soc.* **1960**, *82*, 358.

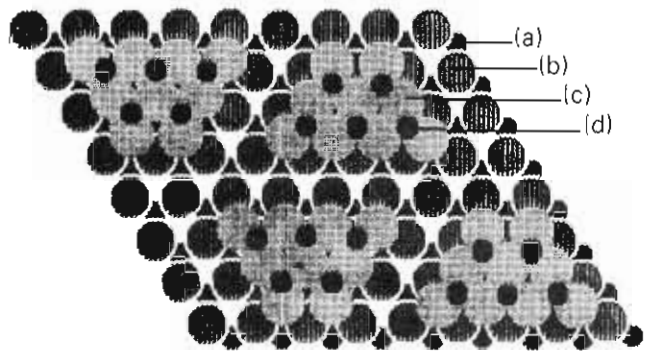

Figure 7. Model of $Mg_{12}Al_6(OH)_{36}(V_{10}O_{28})$ viewed normal to the brucite layers. Atom types are as follows: (a) Mg or Al; (b) OH group in the brucite layer; (c) O from the $V_{10}O_{28}^{6-}$ pillar in contact with the brucite layer; (d) V. (Model was constructed by using Chem-X, developed and distributed by Chemical Design Ltd., Oxford, England.)

hydrotalcite case (Figure 5), results for the isopolymetalate-pillared hydrotalcites are good considering the small number of observed X-ray diffraction lines.

Figure 6 illustrates the thermal behavior of a heptamolybdate-pillared hydrotalcite clay sample. Weight loss at temperatures less than 300–350 °C is due to interlayer water loss, whereas weight loss above this temperature range is attributed to brucite layer dehydroxylation.[14] The large exotherm at 580 °C marks a phase change to α-$MgMoO_4$ and spinel. Decavanadate-pillared hydrotalcite exhibits very similar thermal behavior. Since the hydrotalcite structure is well maintained up to 550–600 °C for isopolymetalate-pillared hydrotalcite, these novel materials should find utility in catalytic applications including base-catalyzed condensations and oxidations.[8,13,14]

Although isopolymetalate-pillared hydrotalcites lose significant amounts of water upon calcination (500 °C/air/12 h), the resulting products show little gain in surface area. By construction of idealized models of these materials, it can be shown that the space between adjacent isopolymetalate pillars is barely large enough for interlayer water molecules (Figure 7). Assuming that the pillars are less than idealy distributed, especially after calcination, voids in the interlayer region of the calcined clay may be difficult if not impossible to access due to pore blockage. Further studies are in progress to try to better understand the properties of the calcined polyoxometalate-pillared hydrotalcite materials.

Conclusion. Isopolymetalate-pillared hydrotalcite clays are easily synthesized by acidification of terephthalate-pillared hydrotalcite in the presence of the appropriate metalate salt (Figure 2). This method affords multihundred-gram samples of pure product by means of a very simple exchange procedure. The heptamolybdate- and decavanadate-pillared hydrotalcites described in this paper are stable above 500 °C. The potential catalytic utility of these robust materials is currently being investigated.

Acknowledgment. Technical assistance by W. J. Dangles and P. A. Shope has been greatly appreciated. I also thank J. A. Kaduk (XRD), J. B. Hall and P. Hruskoci (SEM, TEM), and B. L. Meyers (DTA/TGA) for helpful analysis-related discussions. A. Clearfield and A. K. Cheetham provided useful discussions on various aspects of this work. Helpful comments by the reviewers were appreciated. Finally, I wish to thank the Amoco Chemical Co. for permission to publish this work.